Contact Guidance of Connective Tissue Fibroblasts on Submicrometer Anisotropic Topographical Cues Is Dependent on Tissue of Origin, β1 Integrins, and Tensin-1 Recruitment
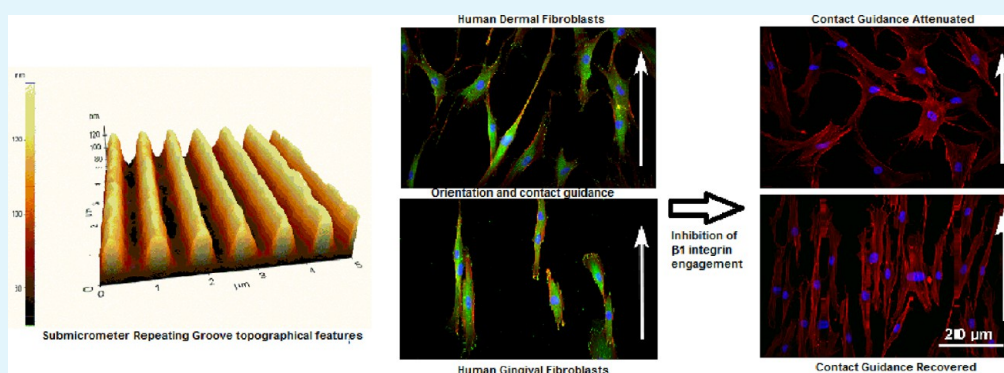
Sarah Brooks, Silvia Mittler, and Douglas W. Hamilton*

Read Online

ACCESS | Metrics & More | Article Recommendations

ABSTRACT: The substratum topography of both natural and synthetic materials is a prominent regulator of cell behaviors including adhesion, migration, matrix fibrillogenesis, and cell phenotype. Connective tissue fibroblasts are known to respond to repeating groove topographical modifications by aligning and exhibiting directed migration, a phenomenon termed contact guidance. Although both reside in collagen rich connective tissues, dermal and gingival fibroblasts are known to exhibit differences in phenotype during wound healing, with gingival tissue showing a fetal-like scarless response. Differences in adhesion formation and maturation are known to underlie both a scarring phenotype and cell response to topographical features. Utilizing repeating groove substrates with periodicities of 600, 900, and 1200 nm (depth, 100 nm), we investigated the roles of integrins $\alpha v \beta 3$ and $\beta 1$ associated adhesions on contact guidance of human gingival (HGFs) and dermal fibroblasts (HDFs). HGFs showed a higher degree of orientation with the groove long axis than HDFs, with alignment of both vinculin and tensin-1 evident on 600 and 900 nm periodicities in both cell types. Orientation with grooves of any periodicity in HGFs and HDFs did not alter the adhesion number or area compared to smooth control surfaces. Growth of both cell types on all periodicities reduced fibronectin fibrillogenesis compared to control surfaces. Independent inhibition of integrin $\alpha v \beta 3$ and $\beta 1$ in both cell types induced changes in spreading up to 6 h and reduced alignment with the groove long axis. At 24 h post-seeding with blocking antibodies, HGFs recovered orientation, but in HDFs, blocking of $\beta 1$, but not $\alpha v \beta 3$ integrins, inhibited alignment. Blocking of $\beta 1$ and $\alpha v \beta 3$ in HDFs, but not HGFs, inhibited tensin-1-associated fibrillar adhesion formation. Furthermore, inhibition of $\beta 1$ integrins in HDFs, but not HGFs, resulted in recruitment of tensin-1 to $\alpha v \beta 3$ focal adhesions, preventing HDFs from aligning with the groove long axis. Our work demonstrates that tensin-1 localization with specific integrins in adhesion sites is an important determinant of contact guidance. This work emphasizes further the need for tissue-specific biomaterials, when integration into host tissues is required.

**KEYWORDS:** *submicrometer topography, directed migration, fibroblasts, fibrillar adhesion, wound healing*

■ INTRODUCTION

Promoting advantageous cell response in wound healing and biomaterial integration remains a key aspect determining restoration of tissue architecture and function. It has long been recognized that a topographic modification of a biomaterial surface is an effective method for manipulating, and controlling, cell phenotype, especially when considering that the extracellular matrix (ECM) structure itself imparts various topographical cues to cells during development as well as in normal
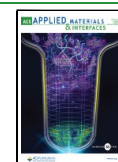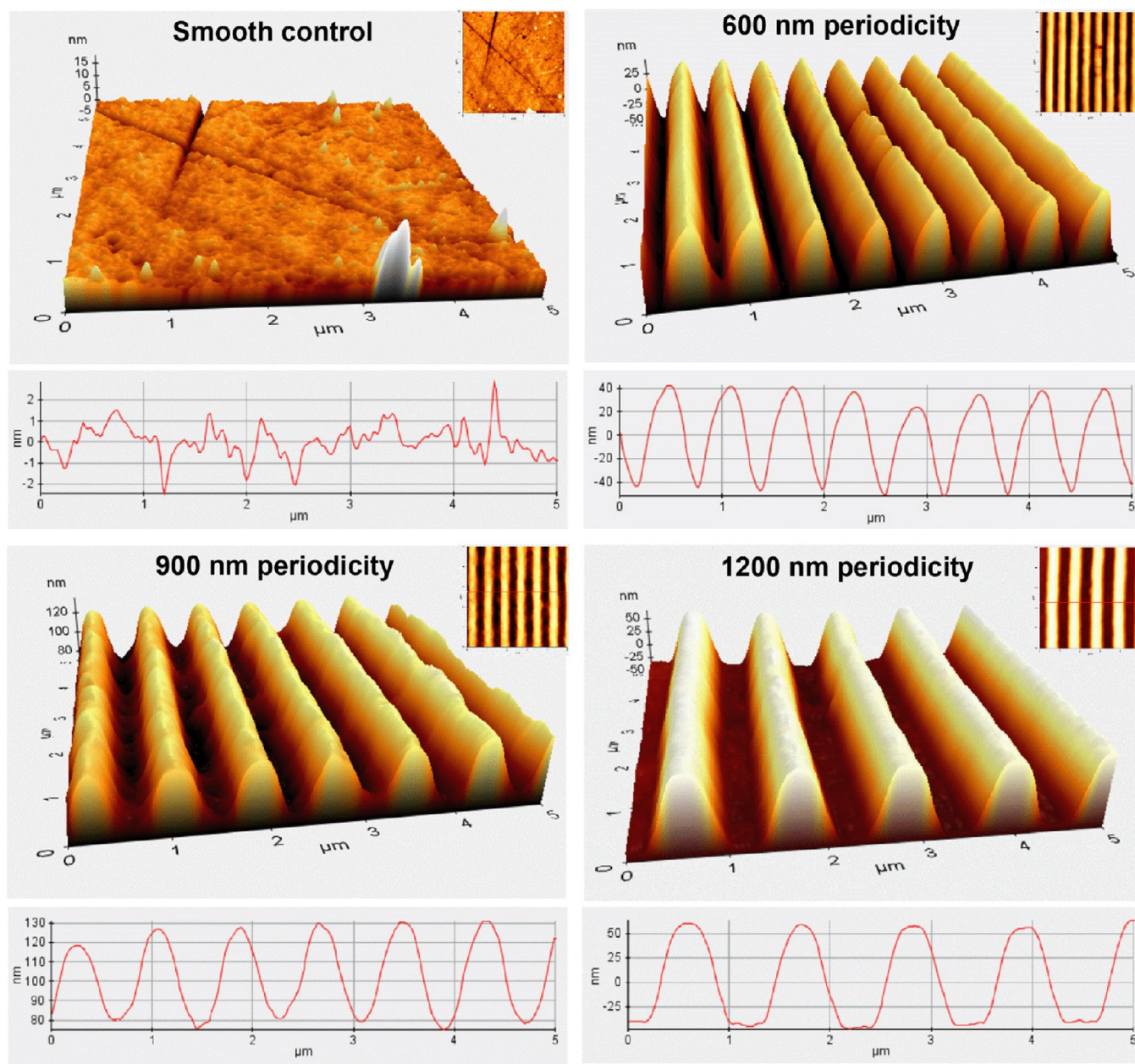
Figure 1. Atomic force microscopy (dynamic mode) images of the ridge/peak profiles of repeating groove topographical cues fabricated in fused silica.

tissue homeostasis.[1,2] Adhesion formation and composition, cell morphology, migration, proliferation and differentiation, and matrix assembly are strongly influenced by topographical cues irrespective of whether a material is natural or artificial.[3,4]

The process of contact guidance is the phenomenon by which cells sense and respond to the underlying topographic and/or chemical characteristics of the culture substratum, characterized by morphological changes, orientation, and directed migration.[5] Despite being well described, the mechanisms resulting in contact guidance remain poorly defined at the molecular level. Initial theories focused on the ″bendability″ of cytoskeletal components,[6] but the advent of submicrometer surfaces demonstrated that biomechanical limitations of F-actin alone could not account for cellular orientation and directed migration. Other research has implicated localized deformation of the cell membrane, local actin accumulation, and topographic discontinuity, but it is generally accepted that filopodia

extension and focal adhesion stability are extremely important in the process.[7−10] Using fibronectin lines, recent research suggests that cells minimize adhesion formation on nonadhesive areas, and that contact guidance is an entropy-driven process.[11,12] However, no unified hypothesis on contact guidance has yet emerged, although it is generally observed that focal adhesion formation occurs prior to cytoskeletal reorganization and is likely a significant driver of the phenomena.[8,13]

While much attention has focused on focal complexes and focal adhesions as drivers of contact guidance, very limited research has addressed the impact of fibrillar adhesion formation on contact guidance and overall cell response to substratum topography. Defined as supermature adhesions, and associated with $\beta 1$ integrins and tensin-1, fibrillar adhesion sites are involved in fibronectin fibrillogenesis, required in tissue repair, and in contact guidance.[14] With respect to the role of fibrillar

Table 1. Root Mean Square Roughness (nm) and Contact Angle (°) of Experimental Periodic Grooved Topographic Surfaces as Determined by Atomic Force Microscopy and Sessile Drop Goniometry

	flat control	600 nm groove	900 nm groove	1200 nm groove
root mean square roughness (nm)	1.19 ± 0.26	28.83 ± 0.07	36.05 ± 0.01	40.27 ± 0.42
contact angle (°)	73.23 ± 4.70	66.93 ± 5.69	70.34 ± 6.00	58.63 ± 7.41

adhesions in cell response to topography, we have previously shown that tensin-1 alignment with respect to the groove long axis is evident in human gingival fibroblasts (HGFs) cultured on repeating microgrooves of 30 μm pitch and 3 μm depth.[15] As cells exhibit contact guidance on this type of topography, it is intuitive that fibrillar adhesions are involved in the process. Further evidence, although indirect, through assessment of fibronectin organization suggests fibrillar adhesions are influenced by topographical cues, but a direct test of their involvement in contact guidance has not been performed.[16]

We hypothesized that β1 integrin and their association with tensin-1 linked fibrillar adhesions are required for contact guidance of connective tissue fibroblasts on submicrometer repeating groove topographies. We demonstrate that while all periodicities of grooves are effective at aligning focal and fibrillar adhesions, culture of dermal and gingival fibroblasts on submicrometer grooves disrupts fibronectin fibrillogenesis. Blocking of β1 and αvβ3 integrins revealed a critical requirement of β1 integrins in contact guidance of dermal but not gingival fibroblasts. Inhibition of β1 integrin engagement in HDFs resulted in recruitment of tensin-1 to focal adhesions, reducing turnover and inhibiting alignment of cells. Of potential significance, the need for β1 integrins in contact guidance of HDFs is dependent on their association with tensin-1 in fibrillar adhesions. Although further research is required, our findings suggest that submicrometer grooved topographies could be used to alter matrix deposition while promoting contact guidance of connective tissue fibroblasts.

■ MATERIALS AND METHODS

Dermal and Gingival Fibroblast Isolation and Culture. Isolation and experimental use of cells derived from human tissue were approved by the Western University Review Board for Health Sciences Research Involving Human Subjects and were in accordance with the 1964 Declaration of Helsinki. Human dermal fibroblasts (HDF) were isolated from skin removed under informed consent from patients undergoing elective lower limb amputation at Victoria Hospital, London, ON, Canada. Human gingival fibroblasts (HGF) were isolated from patients undergoing elective periodontal procedures in the Oral Surgery Clinic at the Schulich School of Medicine and Dentistry, University of Western Ontario, London, ON, Canada. Human dermal and gingival fibroblast populations, each from three different patients, were used up to passage 6 and were maintained in Dulbecco's modified Eagle medium (DMEM; Thermo Fisher Scientific, Burlington, ON, Canada) supplemented with 10% fetal bovine serum (FBS; Gibco Life Technologies, Burlington, ON, Canada) and 1% antibiotics and antimycotic (AA) solution (Gibco Life Technologies, Burlington, ON, Canada) in a humidified environment at 37 °C, 5% CO_2. Media was changed every 2−3 days. Prior to experimental use, the cells were placed in serum free, high glucose DMEM supplemented with 1% AA and maintained at 37 °C, 5% CO_2 for 24 h.

Fabrication of Topographical Cues. In this study, grooved topographical surfaces were fabricated in fused silica by Dr. Erden Ertorer, using HeCd laser nanolithography.[17] The topographical features had periodicities of 600, 900, or 1200 nm with a depth of ∼100 nm. Complete characterization of the topographical features is shown in Figure 1 and Table 1.

Atomic Force Microscopy. Atomic force microscopy was performed by Dr. Heng-Yong Nie at Surface Science Western using a Park Systems XE-100. The surface morphology was imaged with the dynamic force mode using a silicon cantilever having a nominal spring constant of 40 N/m and resonant frequency of 325 kHz. The radius of the apex of the AFM tip at the free end of the cantilever was nominally 8 nm. The AFM images were obtained in air at 256 256 pixels.

Sessile Drop Goniometry. Sessile drop goniometry was performed by Dr. Heng-Yong Nie at Surface Science Western using a DSA30E Drop Shape Analyzer (KRÜSS). A total of 2 μL of ultrapure water was used to measure the contact angle upon all surfaces.

Nanotopographical Substrate Cell Culture. All topographies were sterilized with argon plasma prior to cell seeding. HGFs and HDFs were removed from their growth surfaces using trypsin (0.5%) (Gibco). Cells were seeded on each of the surfaces at a density of 5000 cells/cm², allowed to adhere for 30 min, and flooded with DMEM containing 10% FBS and 1% AA. The cells were maintained in a humidified environment at 37 °C, 5% CO_2. To examine the effect of integrin αvβ3 and integrin β1 upon HGF and HDF adhesion and alignment, inhibitory antibodies against anti-integrin αvβ3 (MAB1976Z; Millipore Sigma, Oakville, ON, Canada), anti-integrin β1 (MAB2253; Millipore Sigma), and control IgG were added to independent cell suspensions at 25 μg/mL. The suspensions were incubated at 37 °C, with gentle agitation, for 30 min prior to seeding as described above.

Adhesion Formation and Extracellular Matrix Deposition Analysis. Cells were fixed with 4% paraformaldehyde for 5 min, rinsed in 1X phosphate buffered saline, incubated within 0.1% Triton X-100 solution for 5 min, rinsed, and blocked by a 1% bovine serum albumin solution (Millipore Sigma) for 30 min. Focal adhesions were visualized using antibodies specific for vinculin (MAB3574; Millipore Sigma) and integrin αvβ3 (MAB1976Z; Millpore Sigma). Fibrillar adhesions were identified using specific antibodies to tensin-1 (NBP1−84129; Novus biologicals, Toronto, ON), integrin β1 (MAB17781; R&D Systems, Minneapolis, MN), and integrin α5 (ab150361; Abcam, Waltham, MA). Extracellular matrix deposition was identified using antibodies to fibronectin (ab1954; Abcam, Waltham, MA). F-actin was labeled with rhodamine conjugated phalloidin (R415; Life Technologies, Grand Island, New York), and nuclei were counterstained with Hoechst (H3560; Invitrogen, Burlington, ON). Images were taken on a Carl Zeiss Axio Imager M2m microscope (Zeiss Microscopes, North York, ON) under reverse osmosis water immersion and processed using Zen Pro software.

Focal and Fibrillar Adhesion Quantification. Immunofluorescent images of HDF and HGF cell populations on each experimental surface were imported into ImageJ. For each stain, a threshold (maximum pixel intensity for each individual dye) was applied to segment regions of interest, and the area was calculated with data points imported into Graphpad Software v.5 (Graphpad Software, La Jolla, CA, USA) for analysis. The overall planar cell area was measured from tracing the borders of F-actin labeling. Cell circularity was also determined with F-actin labeling and applying the circularity formula $[4\pi(\text{area}/\text{perimeter}^2)]$, whereby a value of 1.0 indicates a perfect circle and approaches 0.0 with increasingly elongated structures. The focal adhesion site area was determined using vinculin labeling, and the fibrillar adhesion site area was determined by tensin-1 labeling. These focal and fibrillar adhesion sites were identified within the cell boundary, and the total number and area were normalized to the planar cell area. Directionality of focal and fibrillar adhesion protein complexes, as well as F-actin cytoskeletal organization, was determined through Fourier transform analysis of pixelated segments within each cell or the image frame in the case of fibronectin (Directionality plug in; Fiji; Ashburn, VA, USA). These segments are mapped on a coordinate
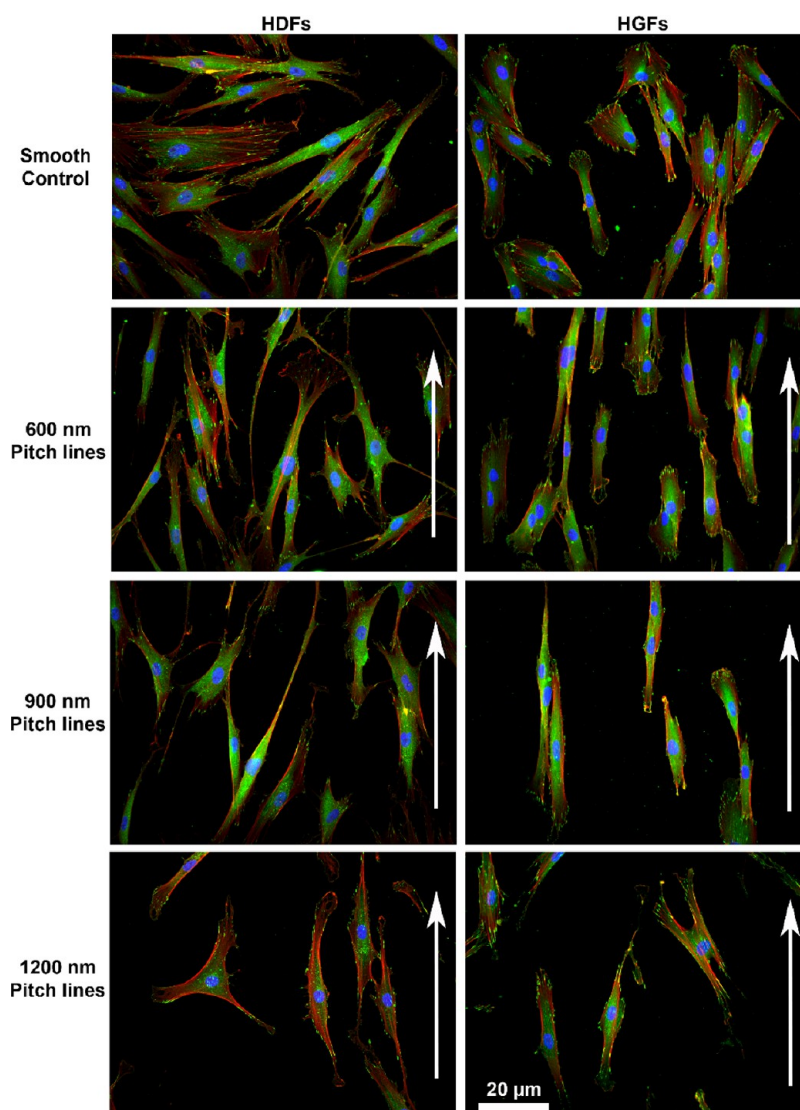
Figure 2. HDFs and HGFs orient with respect to the long axis of the groove topographies. HDF and HGF cell populations were cultured for 24 h upon smooth and groove surfaces with periodicities of 600, 900, and 1200 nm. Vinculin (green), F-actin (red), and nuclei (blue) are identified through immunofluorescent staining. The direction of the underlying nanogroove long axis is indicated with white arrows.

system and directionality determined based upon similar frequency in a direction indicated upon the coordinate system from −90 to 90° in 2° bins. These bins were joined to 10° separation for statistical analysis. The same procedure was repeated for experiments where cells were treated with blocking antibodies for integrin $\alpha v\beta 3$, integrin $\beta 1$, and control IgG.

Statistical Analysis. In all experiments, three separate lines of HDFs and HGFs isolated from different individuals were used. The quantification of adhesion sites for quantity and size was made from a minimum of 10 cells per experiment from three different lines. Results were entered into Graphpad for one-way ANOVA, followed by a Bonferroni correction. Directionality quantification of adhesion sites and the F-actin cytoskeletal element were performed on 10 cells from three independent cell lines of both HDF and HGF cell populations. Fibronectin deposition directionality was quantified on three surface images obtained from three independent cell lines of both HDF and HGF cell populations. The Komolgorov−Smirnov test was used to identify statistical significance of directionality between control conditions and experimental conditions. The quantification of cell area and circularity was made from 10 cells, repeated for three independent cell lines of both HDF and HGF cell populations for each time point and condition. Results were entered into Graphpad Software v.5 for Two-way ANOVA, followed by a Bonferroni correction. For all statistical analyses, $P \leq 0.05$ was considered significant.

RESULTS

Submicrometer Repeating Grooves Induce Alignment of Vinculin, Tensin-1, and F-Actin in HDFs and HGFs without Altering Adhesion Site Quantity or Area. To investigate the influence of submicrometer repeating grooved topographies upon focal adhesion, fibrillar adhesion, and cytoskeletal formation and organization, HDF and HGF were labeled for vinculin, tensin-1, and F-actin with orientation calculated relative to the long axis of the groove. All grooved surfaces imparted linear directionality to HDF and HGF morphology as assessed through alignment of vinculin and F-actin relative to cells cultured on smooth control surfaces (Figure 2). Periodicity grooves (900 nm) were observed to exert the strongest directional cue with respect to the orientation of vinculin, tensin-1, and F-actin in both HDF and HGF (Figure 3). Quantification of alignment using Fournier transform analysis demonstrated that all of the tested groove dimensions influenced alignment of vinculin, tensin-1 (Figure 4), and F-
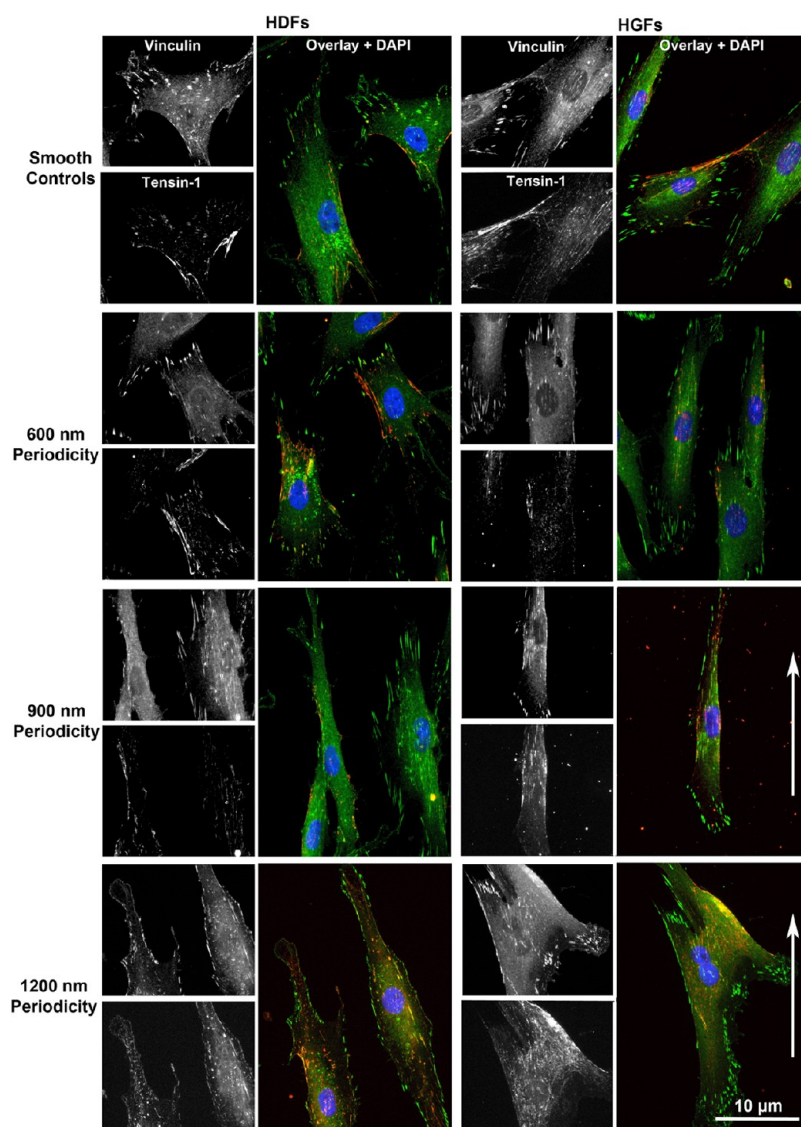
Figure 3. Nanogrooves affect the adhesion site arrangement of HGFs and HDFs. Immunofluorescent staining of vinculin (green), tensin-1 (red), and nuclei (blue) in HDF and HGF populations following a 24 h timepoint upon smooth and groove surfaces. The direction of the underlying nanogroove long axis is indicated with white arrows.

actin depending on the groove periodicity and cell type (Figure 5). In HGFs, vinculin was significantly aligned on all tested periodicities compared to smooth controls ($p < 0.05$, Kolmogorov−Smirnov test), tensin-1 adhesion sites only significantly aligned on 600 and 900 nm ($p < 0.05$, Kolmogorov−Smirnov test), and F-actin aligned on 600 and 1200 nm ($p < 0.05$, Kolmogorov−Smirnov test). In HDFs, vinculin was only significantly aligned on 900 nm periodicity ($p < 0.05$, Kolmogorov−Smirnov test), and tensin-1 sites and F-actin significantly oriented on 600 and 900 nm periodicities ($p < 0.05$, Kolmogorov−Smirnov test). Quantification of vinculin containing focal adhesions and tensin-1 containing fibrillar adhesion site quantity and area normalized to individual HGF and HDF area (Tables 2 and 3) indicated minimal change in size across the investigated topographies when compared to the smooth control ($p < 0.05$, ANOVA, Bonferroni correction).

Fibronectin Deposition and Organization. As fibronectin deposition requires formation of fibrillar adhesion, we next assessed HDF and HGF fibronectin organization at 24 h post-seeding on all tested surfaces (Figure 6). In general, HGFs

secreted higher amounts of fibronectin on smooth control surfaces than HDFs. On grooves with 600, 900, and 1200 nm periodicities, both HDFs and HGFs show reduced fibronectin fibril formation compared to both cell types cultured on smooth control surfaces, with a more punctate appearance evident on grooves. As fibronectin fibrillogenesis is associated with $\alpha5\beta1$ integrins, using antibodies specific for $\alpha5$ and $\beta1$, we assessed their colocalization and assembly in heterodimers (Figure 7). On smooth surfaces, HDF and HGF integrin $\alpha5$ and $\beta1$ colocalize in long plaque-like adhesion sites, but on all experimental grooved surfaces, although the subunits colocalize, adhesion size was diminished.

Inhibition of Integrin $\alpha v\beta3$ and Integrin $\beta1$ Influence HDF and HGF Spreading. As integrin $\alpha v\beta3$ containing adhesions are associated with initial adhesion and $\beta1$ integrin with more mature fibrillar adhesions, we examined the influence of their inhibition on early spreading events of HDFs and HGFs (Figure 8). Assessment of cell spreading through vinculin and F-actin labeling of HDF and HGF on the 900 nm periodicity groove surface showed altered spreading in both cell
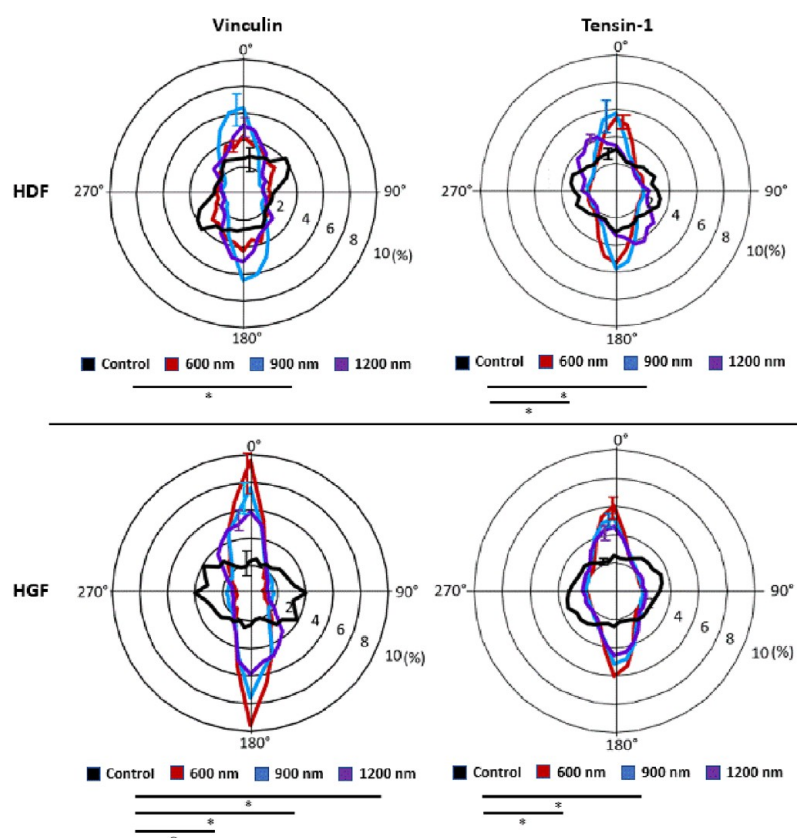
Figure 4. Submicrometer grooves orient HGF and HDF adhesion proteins. Directionality of vinculin and tensin-1 in HDF and HGF fibroblasts at 24 h post-seeding. Mean values established through Fourier transform analysis are displayed in 10° increments ranging from 0 to 360°. The greatest standard deviation at any point of the distribution is displayed. Data were analyzed using the Kolmogorov−Smirnov test of the smooth controls and each experimental surface for both HDF and HGF populations ($N = 3$; *$P < 0.05$).

populations. Inhibition of both $\alpha v \beta 3$ and $\beta 1$ integrins in HDFs resulted in filopodia extensions around the entire cell edges at 1 h post-seeding (Figure 8A). In contrast, HGFs remained spherical with both $\alpha v \beta 3$ and $\beta 1$ integrin inhibition similar to IgG controls at 1 h. At 3 and 6 h post-seeding, both HGFs and HDFs exhibited increased spreading, but qualitatively, no increased directionality of the cell long axis to the groove long axis was observed. This was particularly evident in HGFs (Figure 8B). Quantification of average cell area demonstrated no significant change is HDFs between the treatment groups (Figure 9A), but circularity was significantly reduced by both $\alpha v \beta 3$ and $\beta 1$ integrin inhibition at 1 and 3 h, but not 6 h post-seeding (Figure 9B). Integrin $\alpha v \beta 3$ and integrin $\beta 1$ inhibition in HGFs had no effect on cell area or circularity at 1 h post seeding (Figure 9C,D). Inhibition of integrin $\alpha v \beta 3$ in HGFs did not significantly alter the average cell area at 6 h post-seeding in two of three cell lines tested (Figure 9C). However, the average circularity of integrin $\alpha v \beta 3$ inhibited HGFs was significantly different from the IgG control in two tested cell lines at 6 h post seeding (Figure 9C).

Inhibition of Integrin $\alpha v \beta 3$ and Integrin $\beta 1$ Reduce HDF Orientation/Alignment, but Not in HGFs at 24 h Post Seeding. HGFs and HDFs were cultured on smooth surfaces or 900 nm grooves with integrin $\alpha v \beta 3$ or integrin $\beta 1$ inhibited (Figure 10). F-Actin labeling demonstrated qualitatively that inhibition of integrin $\beta 1$ and $\alpha v \beta 3$ had a larger influence on HDF directionality that HGFs on 900 nm grooves (Figure 10A). Fourier transform analysis demonstrated a significant reduction in the linear orientation of the cells' long

axis within HDFs when integrin $\beta 1$ ($p < 0.05$), but not $\alpha v \beta 3$ ($p > 0.05$), was inhibited compared to IgG controls (Figure 10B). In contrast, inhibition of $\beta 1$ and $\alpha v \beta 3$ integrins had no effect on the linear orientation of HGFs versus IgG controls ($p > 0.05$) (Figure 10C). Assessment of vinculin (focal adhesions) and tensin-1 (fibrillar adhesions) demonstrated that in HDFs, both $\alpha v \beta 3$ and integrin $\beta 1$ inhibition attenuated fibrillar adhesion formation at 24 h post seeding (Figure 11A). In contrast, in HGFs $\alpha v \beta 3$ and integrin $\beta 1$ inhibition had no effect on fibrillar or focal adhesion formation (Figure 11B). Inhibition of integrin $\beta 1$ in HDFs and HGFs cultured on 900 nm periodicity grooves demonstrated difference in tensin-1 localization (Figure 12). In HDFs, integrin $\alpha v \beta 3$ is observed near the periphery of the cell, colocalized with tensin-1. In contrast, HGFs do not exhibit colocalized tensin-1 and integrin $\alpha v \beta 3$.

■ DISCUSSION

Topographic modification of biomaterials to control cell colonization and tissue integration has been a major research focus driven particularly by the evolution of devices such as dental implants.[18] It is known that cells respond to topographical cues through changes in adhesion, spreading, alignment, and migration, which can subsequently enhance integration of biomaterials into host tissues.[4,19,20] Although topographic modifications for bone interfacing biomaterials have been determined and are used clinically with great success, slower progress has been made in optimal topographic modifications of biomaterials for enhancing repair of soft tissues such as skin and gingiva.[21] Despite residing in tissues with a similar histological
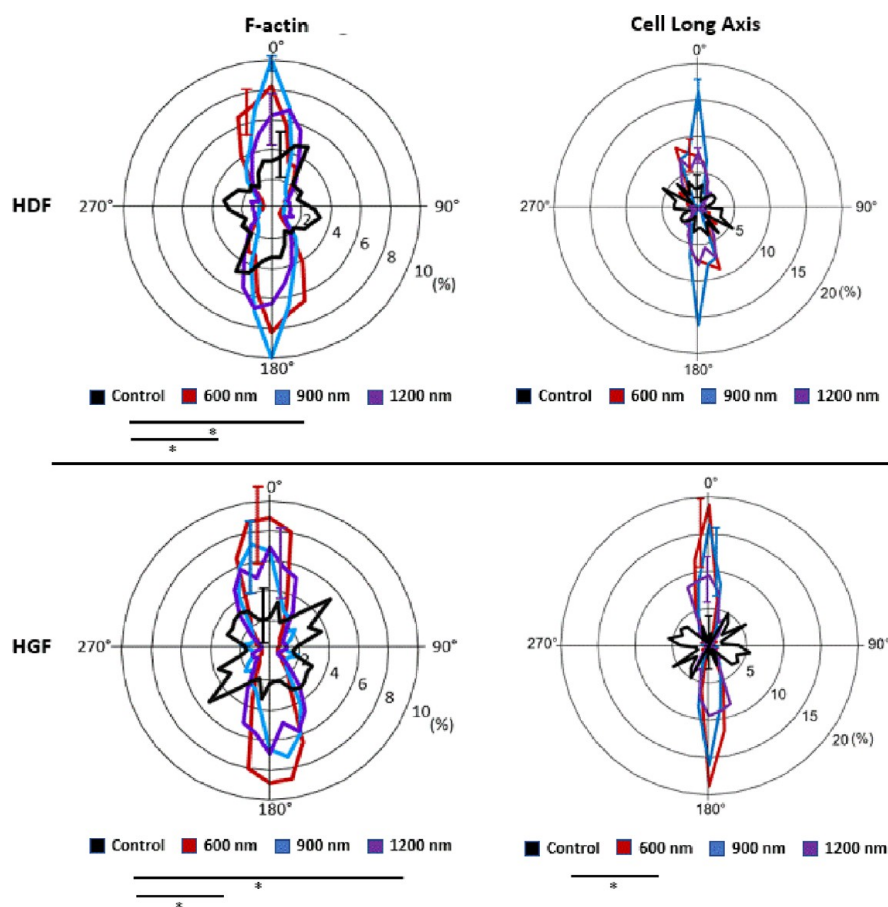
Figure 5. Submicrometer grooves orient HGF and HDF cytoskeletal proteins. Directionality of F-actin and the cellular long axis in HDF and HGF fibroblasts at 24 h post-seeding. Mean values established through Fourier transform analysis are displayed in 10° increments ranging from 0 to 360°. The greatest standard deviation at any point of the distribution is displayed. Data were analyzed using the Kolmogorov−Smirnov test of the smooth controls and each experimental surface for both HDF and HGF populations ($N = 3$; *$P < 0.05$).

Table 2. Average Quantity and Area of Vinculin Containing Focal Adhesions[a]

topography	cell population	average number of adhesions (per μm^2)	average adhesion area (μm^2)
smooth control	HDF	0.033 ± 0.012	2.423 ± 0.998
	HGF	0.022 ± 0.008	2.140 ± 1.106
600 nm groove	HDF	0.032 ± 0.009	1.866 ± 0.709
	HGF	0.026 ± 0.014	2.178 ± 1.204
900 nm groove	HDF	0.039 ± 0.009	2.165 ± 1.101
	HGF	0.027 ± 0.009	1.594 ± 0.586
1200 nm groove	HDF	0.039 ± 0.011	2.267 ± 0.753
	HGF	0.026 ± 0.006	1.738 ± 0.688

[a]Data was analyzed using one way-ANOVA of the smooth controls and each experimental surface for both HDF and HGF populations ($N = 3$; $n = 10$; *$P < 0.05$).

Table 3. Average Quantity and Area of Tensin-1 Containing Fibrillar Adhesions[a]

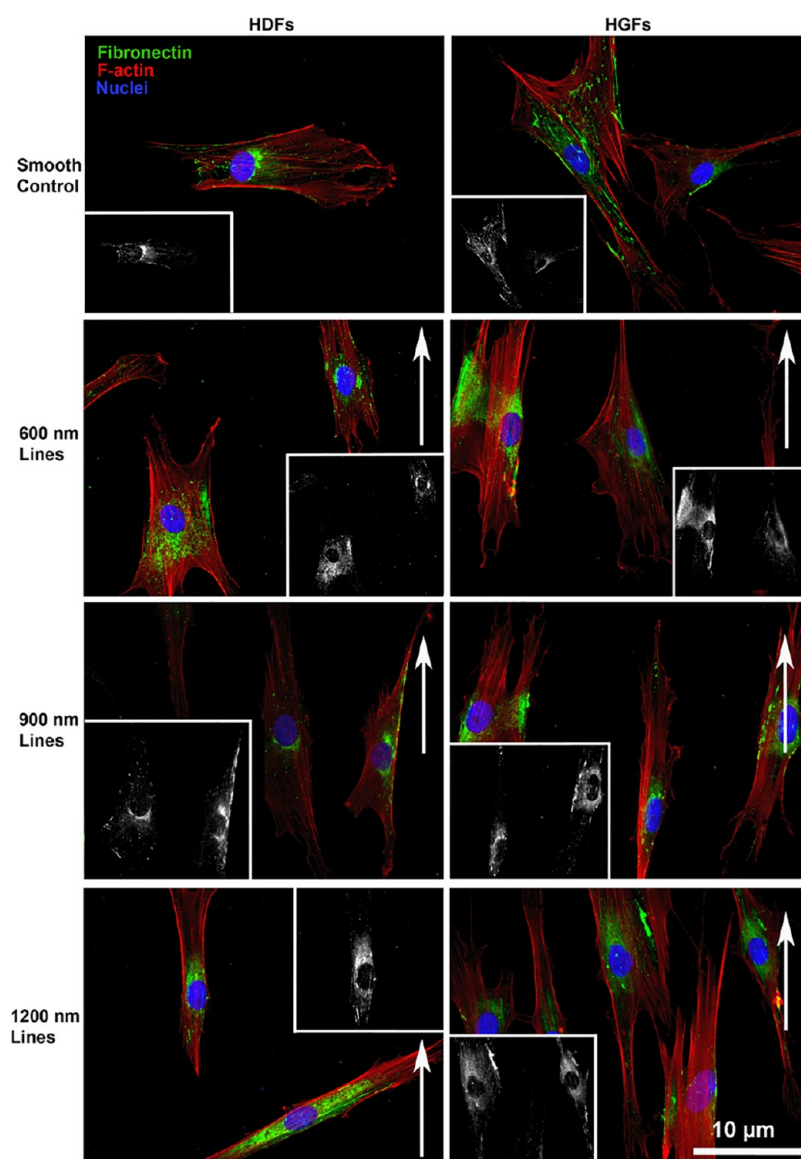| topography	cell population	average number of adhesions (per μm^2)	average adhesion area (μm^2)
flat control	HDF	0.036 ± 0.013	1.905 ± 1.084
	HGF	0.024 ± 0.012	1.707 ± 0.626
600 nm groove	HDF	0.044 ± 0.016	1.343 ± 0.637
	HGF	0.031 ± 0.016	1.323 ± 0.803
900 nm groove	HDF	0.045 ± 0.014	1.138 ± 0.664*
	HGF	0.031 ± 0.014	1.325 ± 1.280
1200 nm groove	HDF	0.040 ± 0.016	1.750 ± 1.305
	HGF	0.027 ± 0.017	1.340 ± 0.586

[a]Data was analyzed using one way-ANOVA of the smooth controls and each experimental surface for both HDF and HGF populations ($N = 3$; $n = 10$; *$P < 0.05$).

topographies on adhesion formation, contact guidance, and fibronectin fibrillogenesis.

HGFs and HDFs Exhibit Morphological and Adhesion Alignment to Submicrometer Groove Topographies. In this study, we utilized submicrometer grooves with varying periodicity as in our previous studies. We determined that periodicity of structures exerted a significant influence in human periodontal ligament (PDL) fibroblasts, orienting adhesion

architecture, fibroblasts originating from gingival tissue are associated with a fetal-like wound healing phenotype compared to dermal fibroblasts, with gingiva exhibiting a propensity toward tissue regeneration rather than scar formation seen in skin.[22] In this study, using both gingival and dermal fibroblasts, we investigated the effect of submicrometer repeating groove
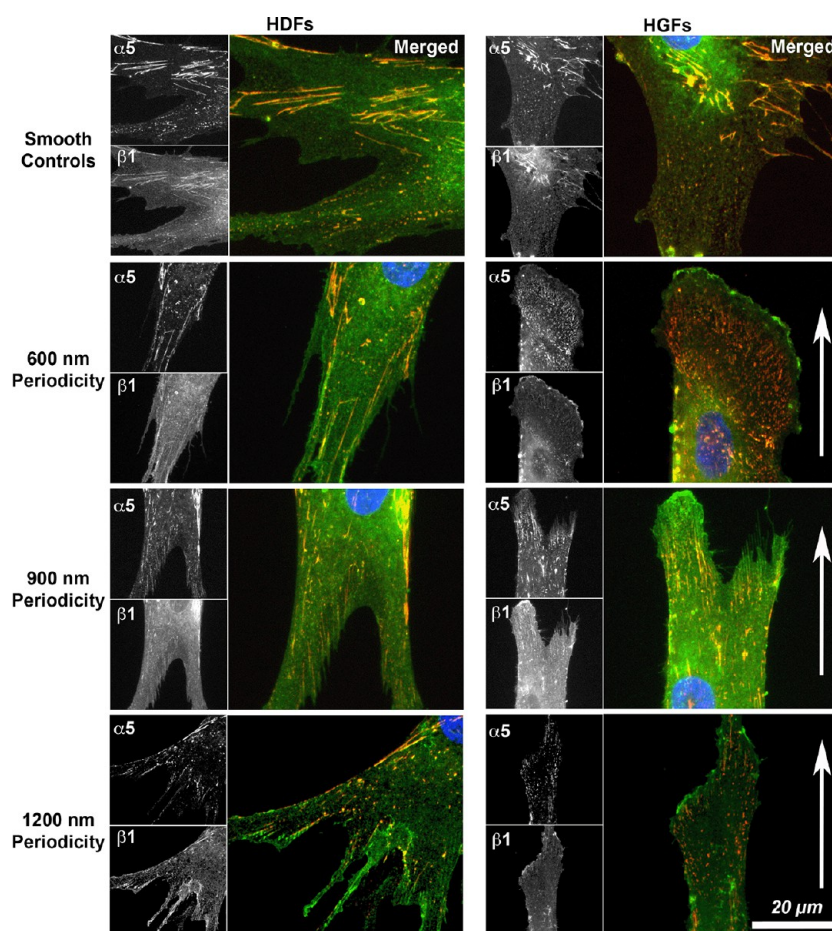
Figure 6. HDF and HGF fibronectin fibril assembly is disrupted by anisotropic repeating groove topographies. Immunofluorescent staining of fibronectin (green), F-actin (red), and nuclei (blue) within HDF and HGF populations following a 24 h timepoint upon the smooth and groove surfaces.

formation and spreading as early as 30 min post-seeding.[8] In addition, cell orientation of PDL fibroblasts to the groove long axis was quantified, with guided migration also evident. Therefore, topographies in the range of 600−900 nm in periodicity and 50−100 nm in depth are sufficient to induce contact guidance by augmenting cellular components and responses rather than the entire cell itself being oriented on a microscale topography. We utilized these surfaces in this study to investigate the response of gingival and dermal fibroblasts. Both HGFs and HDFs aligned to all periodicities of grooves tested compared to smooth control surfaces. Qualitatively, elongation of the cells was most prominent on 600 and 900 nm periodicities compared to 1200 nm, where cells exhibited more spreading perpendicular to the groove long axis. Previous studies have suggested that cell alignment on topographical cue is related to the likelihood of a cell forming stable adhesion sites,[13] with Curtis and Clark hypothesizing that cells form adhesions related to discontinuities such as groove/ridge boundaries.[7] It is conceivable that as the periodicity of the grooves increases to

1200 nm, adhesions sites are less restricted in angle of formation (relative to groove long axis) compared to 600 and 900 nm, which allows stable adhesion formation in a direction other than the groove long axis. We have previously shown in PDL cells that adhesion formation and elongation/orientation is driven primarily by adhesion formation in the presence of a continuous groove edge, and lateral adhesion and spreading is increased if the groove edge is discontinuous. As stable adhesion sites allow formation of the leading filopodia and cell spreading, directed migration would most likely occur in the same direction as the adhesion forms. Indeed, filopodia extensions and focal adhesions have been implicated in the process of contact guidance by us and others.[8,23,24]

One interesting finding of our study is when comparing the response of the two fibroblast populations, HGFs consistently formed fewer adhesion sites than HDFs. Previous studies have highlighted reduced expression of pro-adhesive mRNAs, adherence, and spreading on type I collagen and fibronectin of HGF when compared to HDFs.[25] Our results demonstrate that

Figure 7. Association of α5 and β1 integrin dimers is disrupted on anisotropic repeating groove topographies. Immunofluorescent staining of integrin β1 (green), integrin α5 (red), and nuclei (blue) within HDF and HGF populations following a 24 h timepoint upon the smooth and groove surfaces.

on nanogrooves, HDFs and HGFs maintain this difference in adhesion formation, suggesting intrinsic difference within fibroblast response that are most likely due to the tissue of origin. Based on lineage tracing studies and cell separation,[26,27] it is becoming clear that embryonic origin of cells and the microenvironment of the tissue they reside in confer distinct properties to them, or "intrinsic" characteristics.[28] Intrinsic differences encompass gene expression, epigenetics, signaling molecules, transcription factors, and adhesion.[28] Evidence has previously highlighted that cells align and adhere preferentially to nanogroove topographies of optimal dimensions, specific to the cell type and cell niche.[29] As stated previously, gingival tissue is associated with a scarless response in tissue repair compared to dermal healing.[22] Dermal fibroblast upon activation exhibit an increase in the focal adhesion number and size, which correlates with increased cellular contractility and the differentiation of fibroblasts into myofibroblasts, which subsequently lay down scar tissue.[30] We have previously shown in a rat model that gingival fibroblasts do not transition into myofibroblasts during healing,[31,32] which supports our findings in this paper that it is likely due to these intrinsic differences in adhesion formation linked to tissue of origin.

Most research related to adhesion formation and contact guidance on topographical cues have focused on focal contacts and focal adhesions, with significantly less emphasis placed on fibrillar adhesions. Associated with recruitment of tensin-1 and α5β1 integrin,[33] fibrillar adhesions are also strongly implicated in the process of myofibroblast differentiation, fibronectin

matrix deposition, and crucially, mechanotransduction.[34−36] We show here that tensin-1 alignment with the groove long axis is most pronounced in both HDFs and HGFs on 600 and 900 nm periodicities. Furthermore, fibrillar adhesion sites in HGFs were smaller than those evident in HDFs. Interestingly, we have previously shown on micrometric topographies that HGFs form large and well developed fibrillar adhesions, suggesting a clear difference in adhesion dynamics of HGFs on submicrometer topography.[15] However, it is also logical that in cells that show a propensity toward contractility and myofibroblast differentiation, tensin-1 associated adhesion sites would be more pronounced as is seen in HDFs. Our previous work has shown that submicrometer random cues such as sand-blasted, acid etched topographies that limit available contact area for HGF adhesion formation reduce behaviors associated with fibrosis.[4]

HDFs and HGFs Require both Integrin αvβ3 and Integrin β1 Adhesion Sites for Cell Spreading and Elongation up to 6 h Post-Seeding. As focal and fibrillar adhesions are associated with αvβ3 and α5β1 integrins, respectively, we next investigated what influence their inhibition would have on contact guidance of HDFs and HGFs. Adhesions are considered to form in a hierarchical manner, with focal contacts least mature, followed by focal adhesions and finally formation of the supermature fibrillar adhesions.[37] While derivation of cell lines in which these integrins were genetically deleted would give a more direct measure of their involvement in contact guidance, in this study, we utilized blocking antibodies. As both αvβ3 and β1 integrins are required for development, it
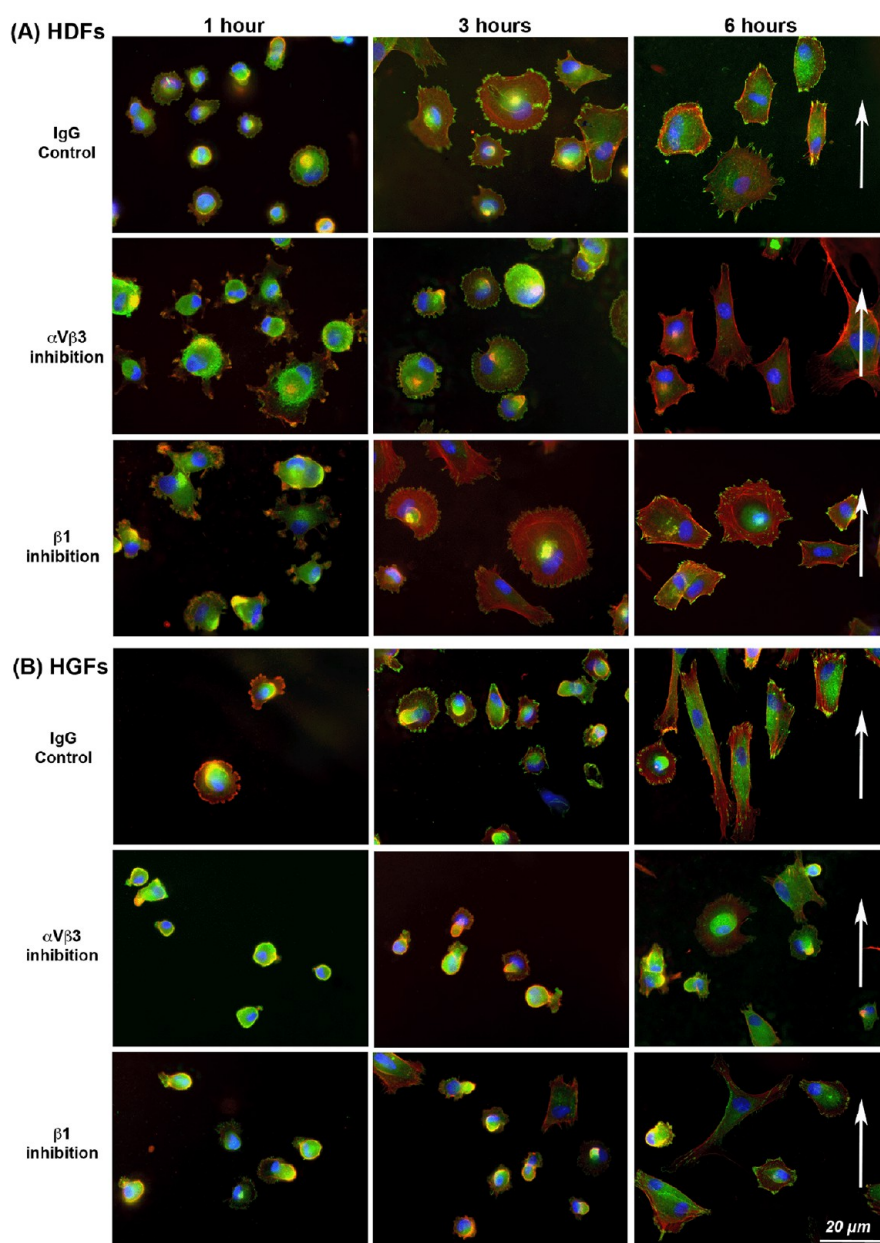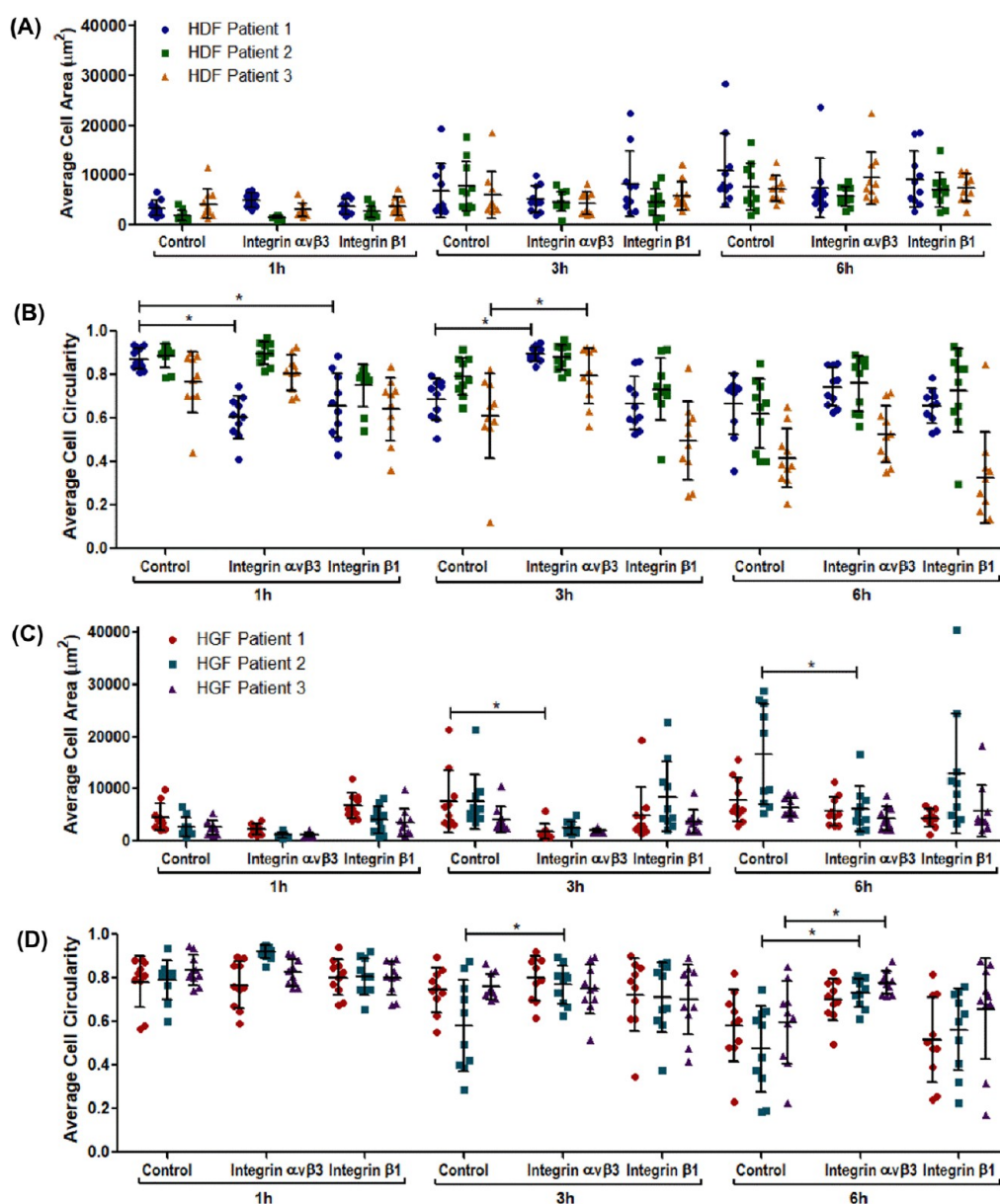
Figure 8. Inhibition of integrin $\alpha v\beta 3$ and integrin $\beta 1$ has a differential effect upon HGF and HDF spreading. Immunofluorescent staining of (A) HDF and (B) HGF vinculin (green), F-actin (red), and nuclei (blue) following 1, 3, and 6 h upon a 900 nm periodicity groove surface. The direction of the underlying nanogroove long axis is indicated by white arrows. Scale bar: 20 μm.

would involve derivation of two separate conditional knockout mice lines to derive appropriate cells. Furthermore, we wanted to make direct comparison between human dermal and gingival fibroblasts, and as inhibition of integrins are removed, it also allowed assessment of how long it took for cells to reorient to the grooves.

With regards to attachment and spreading, inhibition of integrin $\alpha v\beta 3$ and integrin $\beta 1$ in both HGFs and HDFs had little significant impact on circularity or cell area compared to cells on control surfaces. However, assessment of cell morphology demonstrated differences between HGFs and HDFs, with HDFs in particular extending numerous filopodia when either integrin $\alpha v\beta 3$ or integrin $\beta 1$ were blocked at 1 h post-seeding. In contrast, HGFs remained spherical with no spreading evident. Both HGFs and HDFs showed increased spreading at 6 h post-seeding, although orientation with groove long axis was minimal,

particularly for HGFs. Perhaps not surprisingly, inhibition of $\alpha v\beta 3$, but not integrin $\beta 1$, reduces formation of vinculin containing adhesion even 6 h post seeding in HDFs and HGFs. Integrin $\alpha v\beta 3$ has been established as the primary integrin involved in focal adhesion complexes and filopodia extensions but is also a receptor for vitronectin and fibronectin.[38] Previous studies have shown that inhibition of integrin $\alpha v\beta 3$ in oral squamous carcinoma cells eliminates directionality of cell migration on fibronectin matrices.[39] Interestingly, it was also demonstrated that in the presence of DisBa-01 (RGD containing disintegrin), the size and number of paxillin associated adhesions increased in cancer cells of epithelial origin, but no differences were seen in fibroblasts. The inhibition of integrin $\alpha v\beta 3$ should impede filopodia and lamellipodia stability, preventing activation of the mechanosensory pathways that would result in alignment of the cells to the groove long

Figure 9. HDF and HGF cell area and circularity are affected by $\alpha v\beta 3$ and integrin $\beta 1$ blocking antibodies The average HDF (A) and HGF (C) area and HDF (B) and HGF (D) circularity in the presence of integrin $\alpha v\beta 3$ and $\beta 1$ blocking antibodies at 1, 3, and 6 h were quantified. Data is expressed as mean $\pm$ standard deviation. Data was analyzed using two-way ANOVA, followed by Bonferroni post-tests ($N = 3$; *$P < 0.05$).

axis.[8,40] However, the disruption of integrin $\beta 1$ mediated adhesion demonstrates a clear need for fibrillar adhesions in contact guidance and initial alignment of cells to repeating grooves.

Inhibition of Integrin $\alpha v\beta 3$ and Integrin $\beta 1$ Illustrates an Essential Role for $\beta 1$ Integrins in Contact Guidance of HDFs but Not HGFs. With an established short-term effect upon HGF and HDF adhesion and cell spreading as a result of integrin $\alpha v\beta 3$ and integrin $\beta 1$ inhibition, we next investigated the influence of integrin inhibition on cell orientation and adhesion formation at 24 h post-seeding. Assessment of cell alignment to the groove long axis through F-actin labeling revealed that inhibition of $\beta 1$ integrins in HDFs attenuated orientation. Interestingly, we show that at 24 h post-inhibition, HDFs contain minimal fibrillar adhesions when either $\alpha v\beta 3$ or integrin $\beta 1$ are inhibited and the cells do not align to the groove long axis. It provides further evidence of the hierarchical nature

of adhesion formation in HDFs,[37] specifically with the observation that inhibition of $\alpha v\beta 3$ prevents formation of mature fibrillar adhesions. However, the absence of tensin-1 associated fibrillar adhesions in HDFs with either $\alpha v\beta 3$ and or $\beta 1$ integrin establishes that $\beta 1$ is required for alignment and contact guidance. Furthermore, it suggests that it is $\beta 1$ integrins and their association with tensin-1 and fibrillar adhesions that is required. This confirms an essential role for integrin $\beta 1$ in cell response to submicrometer grooves independent of their localization with tensin-1. Of particular significance, it has been previously demonstrated that integrin $\beta 1$ is required for matrix synthesis by dermal fibroblasts, where it is thought to be a primary mechanosensor.[41] As fibrotic encapsulation of materials including breast implants is a major clinical concern, understanding further the role of topography in recruitment of $\beta 1$ integrins and its downstream effects could be of significance in biomaterial design.[42]
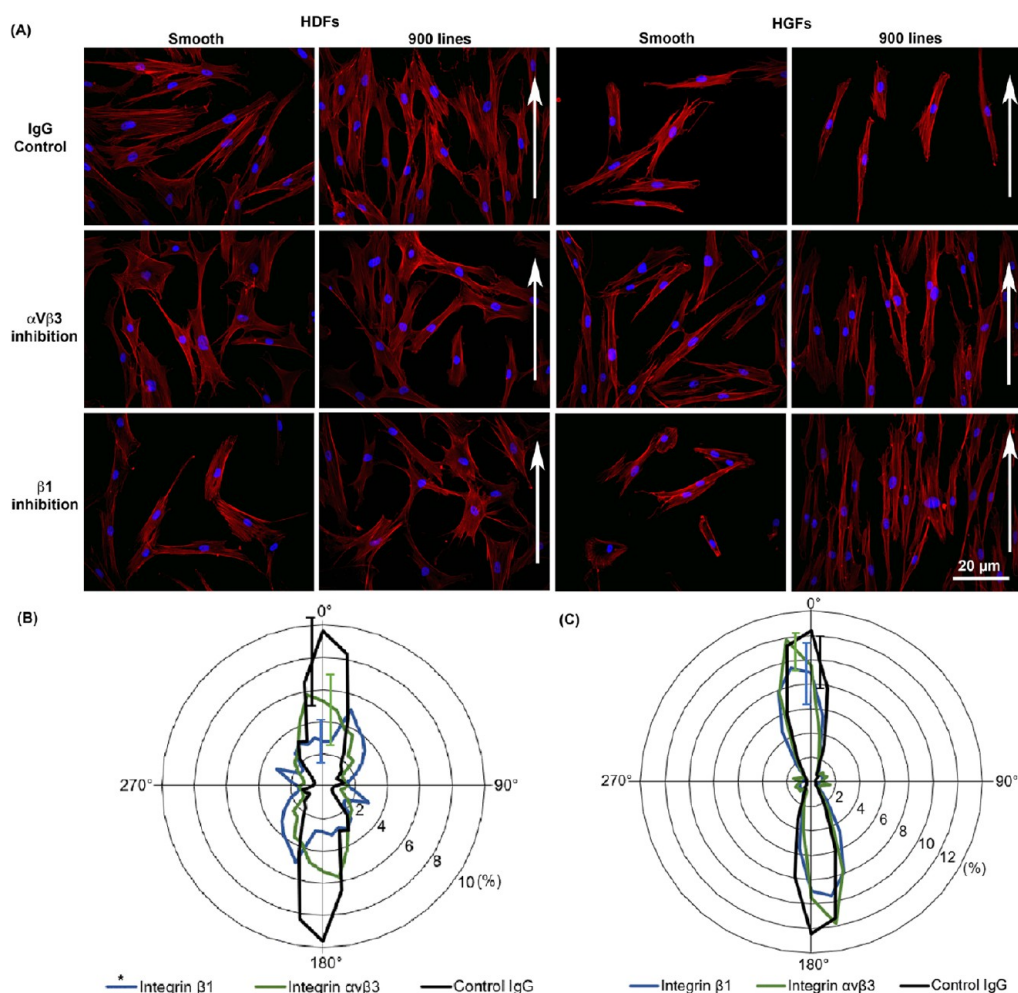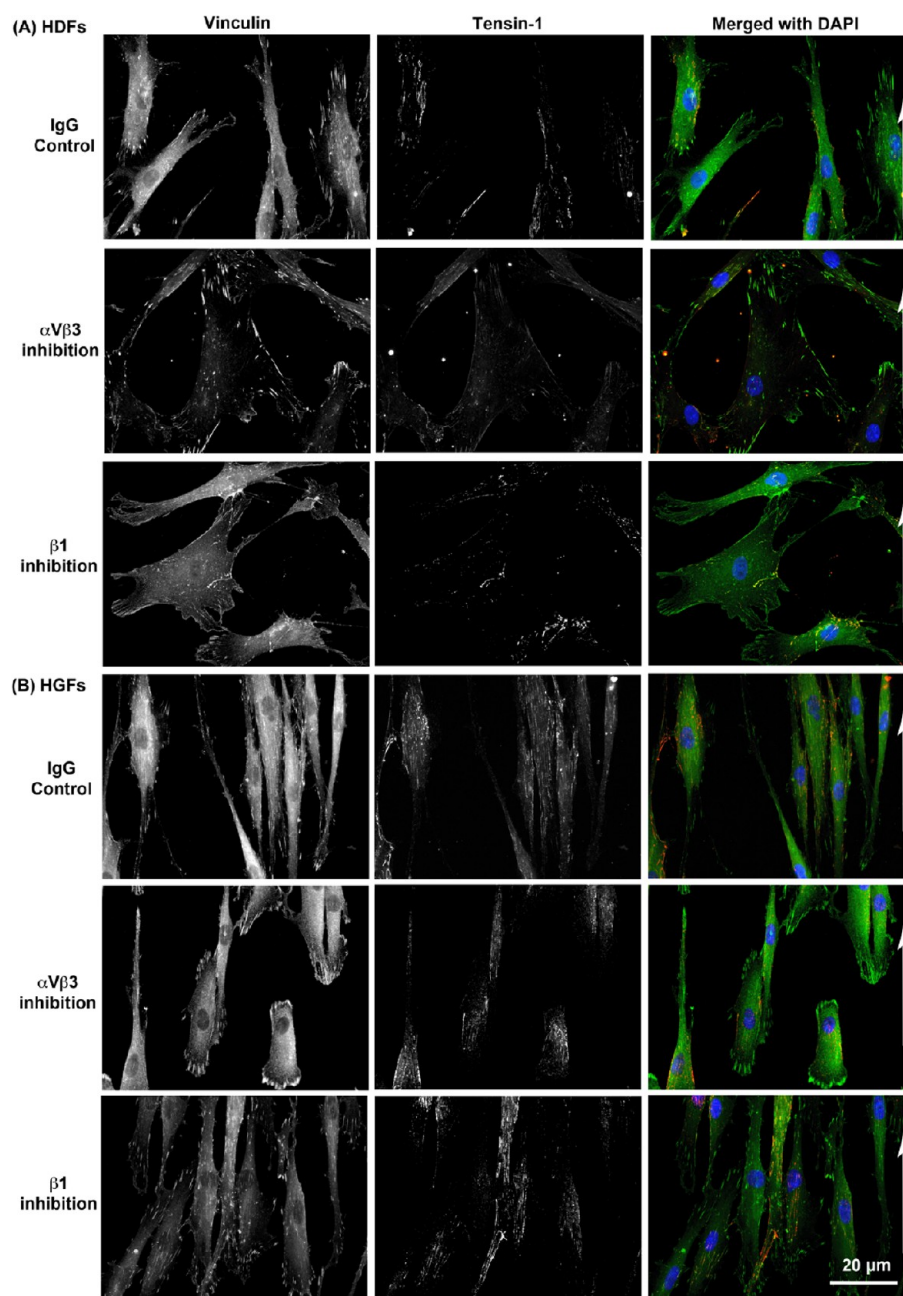
Figure 10. Independent inhibition of integrin $\alpha v\beta 3$ and integrin $\beta 1$ demonstrates contrast in alignment between HDF and HGF. (A) Immunofluorescent staining of F-actin in HDFs and HGFs at 24 h on a 900 nm periodicity groove surface. (B) Directionality of F-actin expression of integrin $\alpha v\beta 3$ and integrin $\beta 1$ inhibited HDF and (C) HGF following a 24 h timepoint. Mean values are displayed in 10° increments ranging from 0 to 360°. The greatest standard deviation at any point of the distribution is displayed. Data was analyzed using the Komolgorov−Smirnov test between each experimental condition and the control IgG treatment for both HDF and HGF populations ($N = 3$; *$P < 0.05$). The direction of the underlying nanogroove long axis is indicated by white arrows.

HDFs are known to be responsive to substratum stiffness, forming large fibrillar adhesions associated with recruitment of $\beta 1$ integrins. In this study, we utilized grooves fabricated in fused silica, which has a tensile strength in the mega-pascal range. It is conceivable that the material stiffness increases the requirement for integrin $\beta 1$ engagement and overrides the orientation signals provided by the grooves. Of potential significance, we have shown previously that HGFs are resistant to forming large adhesions even on materials such as titanium, with a corresponding low level of myofibroblast transition evident.[4] Moreover, we also demonstrated substratum roughness induced nascent adhesion formation in HGFs, which was associated with the upregulation of inflammatory and matrix remodeling genes. Further analysis of how topographical cues and substratum compliance combine to influence cell phenotype will be of great importance, particularly for adhesion mediated events such as myofibroblast differentiation.

HDFs Recruit Tensin-1 to Focal Adhesions in the Absence of $\beta 1$ Integrin Adhesion Sites. As previously described, fibrillar adhesions are classically defined by the presence of tensin-1 and integrin $\alpha 5\beta 1$ largely localized in the center of the cell. Through antibody labeling, we demonstrated that in the presence of

integrin $\beta 1$ inhibition in HDFs, tensin-1 is recruited to and incorporated into the periphery of the cell, where it associates with integrin $\alpha v\beta 3$ adhesion sites. Such a localization of tensin-1 into $\alpha v\beta 3$ focal adhesions in dermal fibroblasts in response to $\beta 1$ integrin inhibition suggests an attempt to increase contractility in the absence of mature fibrillar adhesions. We suggest that it is also the reason why at 24 h post seeding HDFs lacking $\beta 1$ adhesions do not align or exhibit contact guidance with respect to the groove long axis. Tensin-1 associated adhesion is stable and is known to slow migration, which would account for HDFs not realigning with the groove long axis.[33] This alteration in tensin-1 recruitment upon inhibition of $\beta 1$ integrins seen in dermal fibroblasts is not observed in HGFs, emphasizing an intrinsic difference in adhesion assembly on the same topographies. The recruitment of tensin-1 to sites of focal adhesions associated with vinculin, talin, and integrin $\alpha v\beta 3$ has been described previously.[43] These tensin-1 containing focal adhesions were found to have disrupted fibronectin fibrillogenesis unless bound to integrin $\alpha 5\beta 1$ whereby fibronectin was deposited albeit with impaired fibril formation.[43] This observation is similar to our findings using submicrometer grooves as fibronectin fibril formation is attenuated when

Figure 11. Independent inhibition of integrin $\alpha v\beta3$ and integrin $\beta1$ demonstrates a functional disparity among (A) HDF and (B) HGF. Immunofluorescent staining of vinculin (green), tensin-1 (red), and nuclei (blue) within HDF and HGF populations, following a 24 h timepoint, upon a 900 nm periodicity nanogroove surface. The direction of the underlying nanogroove long axis is indicated by white arrows.

compared to cells on smooth controls. In essence, the addition of submicrometer grooves can replicate the disruption of integrin $\beta1$ complexes required for fibronectin fibrillogenesis in HDFs.

Interestingly, neither $\alpha v\beta3$ nor $\beta1$ inhibition prevented alignment of HGFs on 900 nm periodicity grooves at 24 h. However, in contrast to HDFs, in HGFs, tensin-1 labeling is somewhat similar to IgG controls, such that inhibition of $\alpha v\beta3$ and $\beta1$ integrins does not completely inhibit fibrillar adhesion formation at 24 h post seeding. It is conceivable that HGFs are able to turnover integrins faster than HDFs, which would account for the presence of fibrillar adhesions particularly when integrin $\beta1$ is inhibited. However, we also noted a significant difference in $\beta1$ localization in HGFs compared to HDFs,

suggesting that they could be of less importance in adhesion-mediated events in gingival tissue. It does however emphasize that fibroblast populations from different tissues possess different properties and tissue specificity maybe important for the design of biomaterials for soft connective tissues such as skin or gingiva.

Submicrometer Grooves as an Anti-Fibrotic Surface: Disruption of Fibronectin Fibril Formation. Both integrin $\alpha5\beta1$ and $\alpha v\beta3$ integrins are known to bind to fibronectin, with fibrillar adhesion in particular involved in fibronectin fibrillo-genesis.[43] We show here through qualitative evaluation of HDFs and HGFs that the presence of submicrometer grooves disrupts fibronectin fibril formation. Upon the flat control surface, distinct fibrils of fibronectin can be seen under the cell. When
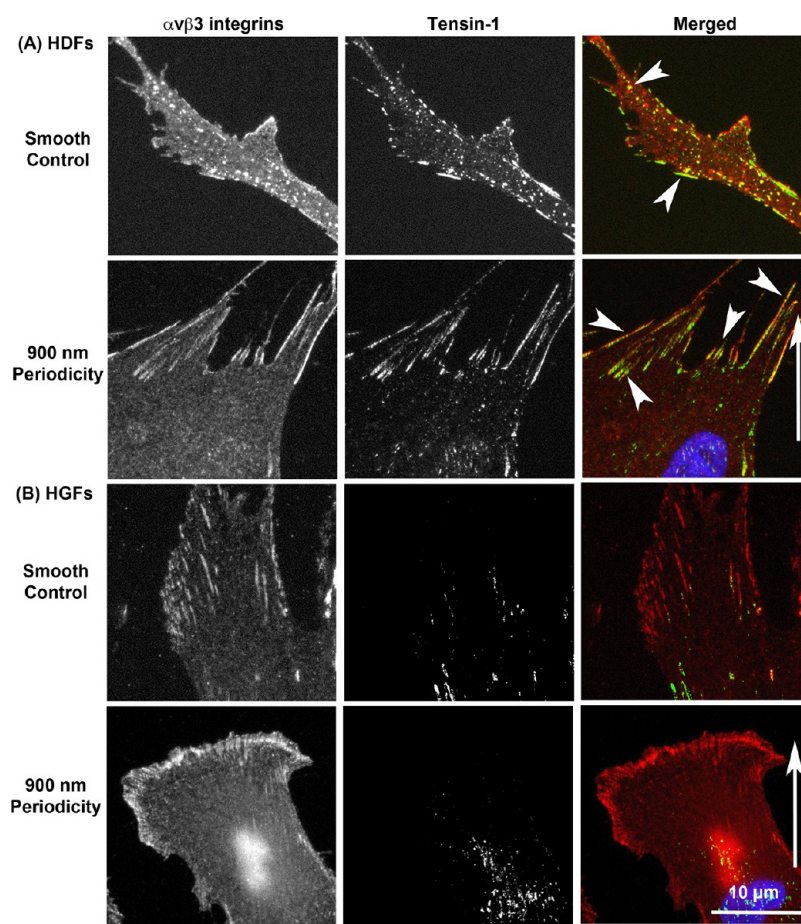
Figure 12. Inhibition of integrin β1 results in tensin-1 recruitment to αvβ3 peripheral adhesion sites in (A) HDFs, but not (B) HGFs. Immunofluorescent staining of tensin-1 (green), integrin β1 (red), and nuclei (blue) within HDF and HGF populations following a 24 h timepoint. The direction of the underlying nanogroove long axis is indicated by white arrows.

cultured on the submicrometer grooves of all periodicities, immunofluorescence shows more punctate fibronectin organization, with fewer fibrils evident. This result is in agreement with previous studies, which indicated a disruption in HGF fibronectin deposition upon roughened titanium surfaces relative to smooth controls.[4]

Biomaterials implanted within native tissues typically invoke a foreign body response, similar to the normal healing response, often resulting in the formation of fibrous or scar tissue around the biomaterial.[44,45] While recent studies have shown that changing the compliance of a material can reduce fibrotic tissue formation,[42] the potential of topographical modifications to reduce matrix production and myofibroblast differentiation on implanted materials is intriguing. This is particularly attractive as topographic modification of biomaterials is usually permanent and could avoid the need for changing the tensile strength of materials, which could preclude their clinical utility. Future studies will assess how our submicrometer grooves influence capsule formation and fibrosis using in vivo models. Of encouragement, using a porcine model, it has been recently demonstrated that fibrotic capsule formation on pacemakers can be reduced by the addition of cellulose fabricated micrometric hexagonal topographic features.[46]

■ CONCLUSIONS

Contact guidance is an important cell phenomenon that permits colonization and integration of biomaterials into host tissues.

The results of this study demonstrate for the first time that β1 integrins are an important determinant of cell alignment to submicrometer grooves in dermal fibroblasts and that fibroblasts isolated from gingiva and dermis exhibit different responses to the same topographies. The finding that fibroblasts with different tissue origins exhibit altered behavior on the same topographies further highlights the specificity requirement in designing materials for augmenting tissue repair. In addition, our findings further highlight the difference in adhesion formation evident between dermal and gingival fibroblasts, which point further at the role of β1 integrins and tensin-1 in the scarring phenotype of skin versus gingiva. Topographical modulation of integrin β1 and tensin-1 may provide new avenues of investigation for inhibiting fibrosis around implanted materials.

■ AUTHOR INFORMATION

Corresponding Author

Douglas W. Hamilton − *School of Biomedical Engineering and Department of Anatomy and Cell Biology, Schulich School of Medicine and Dentistry, Western University, London, ON N6A 5C1, Canada;* ⓘ orcid.org/0000-0002-9798-5197; Email: dhamil2@uwo.ca

Authors

Sarah Brooks − *School of Biomedical Engineering, Western University, London, ON N6A 5C1, Canada*

Silvia Mittler − *School of Biomedical Engineering, Western University, London, ON N6A 5C1, Canada; Department of*

Physics and Astronomy, Faculty of Science, Western University, London, ON N6A 3K7, Canada; orcid.org/0000-0001-8998-1877

Complete contact information is available at:
https://pubs.acs.org/10.1021/acsami.2c22381

Notes
The authors declare no competing financial interest.

REFERENCES

(1) Britland, S.; Morgan, H.; Wojiak-Stodart, B.; Riehle, M.; Curtis, A.; Wilkinson, C. Synergistic and Hierarchical Adhesive and Topographic Guidance of BHK Cells. *Exp. Cell Res.* **1996**, *228*, 313−325.

(2) Lee, I.; Kim, D.; Park, G. L.; Jeon, T. J.; Kim, S. M. Investigation of Wound Healing Process Guided by Nano-Scale Topographic Patterns Integrated within a Microfluidic System. *PLoS One* **2018**, *13*, 1−16.

(3) Brunette, D. M.; Chehroudi, B. The Effects of the Surface Topography of Micromachined Titanium Substrata on Cell Behavior in Vitro and in Vivo. *J. Biomech. Eng.* **1999**, *121*, 49−57.

(4) Kim, S. S.; Wen, W.; Prowse, P.; Hamilton, D. W. Regulation of Matrix Remodelling Phenotype in Gingival Fibroblasts by Substratum Topography. *J. Cell. Mol. Med.* **2015**, *19*, 1183−1196.

(5) Tamiello, C.; Buskermolen, A. B. C.; Baaijens, F. P. T.; Broers, J. L. V.; Bouten, C. V. C. Heading in the Right Direction: Understanding Cellular Orientation Responses to Complex Biophysical Environments. *Cell. Mol. Bioeng.* **2016**, *12*.

(6) Dunn, G. A.; Heath, J. P. A NEW HYPOTHESIS OF CONTACT GUIDANCE IN TISSUE CELLS. *Exp. Cell Res.* **1976**, *101*, 1−14.

(7) Curtis, A. S. G.; Clark, P. The Effects of Topographic and Mechanical Properties of Materials on Cell Behaviour. *Crit. Rev. Biocompat.* **1990**, *5*, 343−362.

(8) Hamilton, D. W.; Oates, C. J.; Hasanzadeh, A.; Mittler, S. Migration of Periodontal Ligament Fibroblasts on Nanometric Topographical Patterns: Influence of Filopodia and Focal Adhesions on Contact Guidance. *PLoS One* **2010**, *5*, No. e15129.

(9) Leclech, C.; Villard, C. Cellular and Subcellular Contact Guidance on Microfabricated Substrates. *Front. Bioeng. Biotechnol.* **2020**, 1198.

(10) Ohara, P. T.; Buck, R. C. Contact guidance in vitro: A light, transmission, and scanning electron microscopic study. *Exp. Cell Res.* **1979**, *121*, 235−249.

(11) Buskermolen, A. B. C.; Suresh, H.; Shishvan, S. S.; Vigliotti, A.; DeSimone, A.; Kurniawan, N. A.; Bouten, C. V. C.; Deshpande, V. S. Entropic Forces Drive Cellular Contact Guidance. *Biophys. J.* **2019**, *116*, 1994−2008.

(12) Buskermolen, A. B. C.; Ristori, T.; Mostert, D.; van Turnhout, M. C.; Shishvan, S. S.; Loerakker, S.; Kurniawan, N. A.; Deshpande, V. S.; Bouten, C. V. C. Cellular Contact Guidance Emerges from Gap Avoidance. *Cell Rep. Phys. Sci.* **2020**, *1*, No. 100055.

(13) Hamilton, D. W.; Brunette, D. M. "Gap Guidance" of Fibroblasts and Epithelial Cells by Discontinuous Edged Surfaces. *Exp. Cell Res.* **2005**, *309*, 429−437.

(14) Barber-Pérez, N.; Georgiadou, M.; Guzmán, C.; Isomursu, A.; Hamidi, H.; Ivaska, J. Mechano-Responsiveness of Fibrillar Adhesions on Stiffness-Gradient Gels. *J. Cell Sci.* **2020**, *133*, 1−11.

(15) Kokubu, E.; Hamilton, D. W.; Inoue, T.; Brunette, D. M. Modulation of Human Gingival Fibroblast Adhesion, Morphology, Tyrosine Phosphorylation, and ERK 1/2 Localization on Polished, Grooved and SLA Substratum Topographies. *J. Biomed. Mater. Res., Part A* **2009**, *91A*, 663−670.

(16) Den Braber, E. T.; de Ruijter, J. E.; Ginsel, L. A.; von Recum, A. F.; Jansen, J. A. Orientation of ECM Protein Deposition, Fibroblast Cytoskeleton, and Attachment Complex Components on Silicone Microgrooved Surfaces. *J. Biomed. Mater. Res.* **1998**, *40*, 291−300.

(17) Ertorer, E.; Vasefi, F.; Keshwah, J.; Najiminaini, M.; Halfpap, C.; Langbein, U.; Carson, J. J.; Hamilton, D. W.; Mittler, S. Large Area Periodic, Systematically Changing, Multishape Nanostructures by Laser Interference Lithography and Cell Response to These Topographies. *J. Biomed. Opt.* **2013**, *18*, 035002-1-35002−035002-1-35008.

(18) Gupta, S.; Dahiya, V.; Shukla, P. Surface Topography of Dental Implants: A Review. *J. dent. Implant* **2014**, *4*, 66.

(19) Hamilton, D. W.; Chehroudi, B.; Brunette, D. M. Comparative Response of Epithelial Cells and Osteoblasts to Microfabricated Tapered Pit Topographies in Vitro and in Vivo. *Biomaterials* **2007**, *28*, 2281−2293.

(20) Prowse, P. D. H.; Elliott, C. G.; Hutter, J.; Hamilton, D. W. Inhibition of Rac and ROCK Signalling Influence Osteoblast Adhesion, Differentiation and Mineralization on Titanium Topographies. *PLoS One* **2013**, *8*, No. e58898.

(21) Devgan, S.; Sidhu, S. S. Evolution of Surface Modification Trends in Bone Related Biomaterials: A Review. *Mater. Chem. Phys.* **2019**, *233*, 68−78.

(22) Fournier, B. P. J.; Larjava, H.; Häkkinen, L. Gingiva as a Source of Stem Cells with Therapeutic Potential. *Stem Cells Dev.* **2013**, *22*, 3157−3177.

(23) Klymov, A.; Bronkhorst, E. M.; Te Riet, J.; Jansen, J. A.; Walboomers, X. F. Bone Marrow-Derived Mesenchymal Cells Feature Selective Migration Behavior on Submicro- and Nano-Dimensional Multi-Patterned Substrates. *Acta Biomater.* **2015**, *16*, 117−125.

(24) Prager-Khoutorsky, M.; Lichtenstein, A.; Krishnan, R.; Rajendran, K.; Mayo, A.; Kam, Z.; Geiger, B.; Bershadsky, A. D. Fibroblast Polarization Is a Matrix-Rigidity-Dependent Process Controlled by Focal Adhesion Mechanosensing. *Nat. Cell Biol.* **2011**, *13*, 1457−1465.

(25) Guo, F.; Carter, D. E.; Mukhopadhyay, A.; Leask, A. Gingival Fibroblasts Display Reduced Adhesion and Spreading on Extracellular Matrix: A Possible Basis for Scarless Tissue Repair? *PLoS One* **2011**, *6*, No. e27097.

(26) Myung, P.; Andl, T.; Atit, R. The Origins of Skin Diversity: Lessons from Dermal Fibroblasts. *Development* **2022**, *149*, dev200298.

(27) Walker, J. T.; Flynn, L. E.; Hamilton, D. W. Lineage Tracing of Foxd1-Expressing Embryonic Progenitors to Assess the Role of Divergent Embryonic Lineages on Adult Dermal Fibroblast Function. *FASEB Bioadv.* **2021**, *3*, 541−557.

(28) Picollet-D'hahan, N.; Dolega, M. E.; Freida, D.; Martin, D. K.; Gidrol, X. Deciphering Cell Intrinsic Properties: A Key Issue for Robust Organoid Production. *Trends Biotechnol.* **2017**, 1035−1048.

(29) Chung, K.; DeQuach, J. A.; Christman, K. L. Nanopatterned Interfaces for Controlling Cell Behavior. *Nano Life* **2010**, *01*, 63−77.

(30) Hinz, B. Formation and Function of the Myofibroblast during Tissue Repair. *J. Invest. Dermatol.* **2007**, *127*, 526−537.

(31) Nikoloudaki, G.; Creber, K.; Douglas, X.; Hamilton, W. Wound Healing and Fibrosis: A Contrasting Role for Periostin in Skin and the Oral Mucosa. *Am. J. Physiol. Cell Physiol.* **2020**, *318*, C1065−C1077.

(32) Kim, S. S.; Nikoloudaki, G. E.; Michelsons, S.; Creber, K.; Hamilton, D. W. Fibronectin Synthesis, but Not α-Smooth Muscle Expression, Is Regulated by Periostin in Gingival Healing through FAK/JNK Signaling. *Sci. Rep.* **2019**, *9*, 2708.

(33) Zamir, E.; Katz, M.; Posen, Y.; Erez, N.; Yamada, K. M.; Katz, B.-Z.; Lin, S.; Lin, D. C.; Bershadsky, A.; Kam, Z.; Geiger, B. Dynamics and Segregation of Cell− Matrix Adhesions in Cultured Fibroblasts. *Nat. Cell Biol.* **2000**, *2*, 191−196.

(34) Bernau, K.; Torr, E. E.; Evans, M. D.; Aoki, J. K.; Ngam, C. R.; Sandbo, N. Tensin 1 Is Essential for Myofibroblast Differentiation and Extracellular Matrix Formation. *Am. J. Respir. Cell Mol. Biol.* **2017**, *56*, 465−476.

(35) Pankov, R.; Cukierman, E.; Katz, B.-Z.; Matsumoto, K.; Lin, D. C.; Lin, S.; Hahn, C.; Yamada, K. M. Integrin Dynamics and Matrix Assembly: Tensin-Dependent Translocation of 5 1 Integrins Promotes Early Fibronectin Fibrillogenesis. *J. Cell Biol.* **2000**, *148*, 1075−1090.

(36) Chen, H.; Duncan, I. C.; Bozorgchami, H.; Lo, S. H. Tensin1 and a Previously Undocumented Family Member, Tensin2, Positively

Regulate Cell Migration. *Proc. Natl. Acad. Sci. U. S. A.* **2002**, *99*, 733–738.

(37) Zaidel-Bar, R.; Cohen, M.; Addadi, L.; Geiger, B. Hierarchical Assembly of Cell-Matrix Adhesion Complexes. *Biochem. Soc. Trans.* **2004**, *32*, 416–420.

(38) Patsenker, E.; Popov, Y.; Stickel, F.; Schneider, V.; Ledermann, M.; Sägesser, H.; Niedobitek, G.; Goodman, S. L.; Schuppan, D. Pharmacological Inhibition of Integrin A$v\beta$3 Aggravates Experimental Liver Fibrosis and Suppresses Hepatic Angiogenesis. *Hepatology* **2009**, *50*, 1501–1511.

(39) Montenegro, C. F.; Casali, B. C.; Lino, R. L. B.; Pachane, B. C.; Santos, P. K.; Horwitz, A. R.; Selistre-De-Araujo, H. S.; Lamers, M. L. Inhibition of A$v\beta$3 Integrin Induces Loss of Cell Directionality of Oral Squamous Carcinoma Cells (OSCC). *PLoS One* **2017**, *12*, No. e0176226.

(40) Wong, S.; Guo, W.-H.; Wang, Y.-L. Fibroblasts Probe Substrate Rigidity with Filopodia Extensions before Occupying an Area. *Proc. Natl. Acad. Sci. U. S. A.* **2014**, *111*, 17176–17181.

(41) Leask, A. Integrin B1: A Mechanosignaling Sensor Essential for Connective Tissue Deposition by Fibroblasts. *Adv. Text. Wound Care* **2013**, *2*, 160–166.

(42) Noskovicova, N.; Schuster, R.; van Putten, S.; Ezzo, M.; Koehler, A.; Boo, S.; Coelho, N. M.; Griggs, D.; Ruminski, P.; McCulloch, C. A.; Hinz, B. Suppression of the Fibrotic Encapsulation of Silicone Implants by Inhibiting the Mechanical Activation of Pro-Fibrotic TGF-β. *Nat. Biomed. Eng.* **2021**, *S*, 1437–1456.

(43) Danen, E. H. J.; Sonneveld, P.; Brakebusch, C.; Fässler, R.; Sonnenberg, A. The Fibronectin-Binding Integrins A5β1 and A$v\beta$3 Differentially Modulate RhoA-GTP Loading, Organization of Cell Matrix Adhesions, and Fibronectin Fibrillogenesis. *J. Cell Biol.* **2002**, *159*, 1071–1086.

(44) Noskovicova, N.; Hinz, B.; Pakshir, P. Implant Fibrosis and the Underappreciated Role of Myofibroblasts in the Foreign Body Reaction. *Cell* **2021**, *10*, 1794.

(45) Witherel, C. E.; Abebayehu, D.; Barker, T. H.; Spiller, K. L. Macrophage and Fibroblast Interactions in Biomaterial-Mediated Fibrosis. *Advanced Healthcare Materials.*; Wiley-VCH Verlag 2019. DOI: 10.1002/adhm.201801451.

(46) Robotti, F.; Sterner, I.; Bottan, S.; Monné Rodríguez, J. M.; Pellegrini, G.; Schmidt, T.; Falk, V.; Poulikakos, D.; Ferrari, A.; Starck, C. Microengineered Biosynthesized Cellulose as Anti-Fibrotic in Vivo Protection for Cardiac Implantable Electronic Devices. *Biomaterials* **2020**, *229*, No. 119583.